Electronic Supplementary Material (ESI) for Journal of Materials Chemistry A.

Supplementary Information

In-situ coating of lithiophilic interphase on a biporous Cu scaffold with vertical microchannels for dendrite-free Li metal batteries

Li-Min Wang, Xiao-Kuan Ban, Zong-Zi Jin, Ran-Ran Peng, Chu-Sheng Chen* and Chun-Hua Chen*

CAS Key Laboratory of Materials for Energy Conversions, Department of Materials Science and Engineering,, University of Science and Technology of China, Hefei 230026, Anhui, China

E-mail: cchchen@ustc.edu.cn; ccsm@ustc.edu.cn

Thermal oxidation process:

Actually, the thermal oxidation of Cu mainly includes the following two steps: $2Cu + 1/2O_2 \rightarrow Cu_2O$; $Cu_2O + 1/2O_2 \rightarrow 2CuO$. It has been reported that Cu is first oxidized to Cu_2O, only when the temperature is above 260 ℃, Cu_2O will further react with oxygen to form CuO.[1] As shown in **Fig. S1**, only a small amount of Cu_2O and no CuO is formed at 250 ℃. At 300 ℃ and higher temperatures, CuO is formed and increases with the temperature, while Cu_2O still occupies a large proportion. CuO can be produced directly only at higher temperatures, however, the scaffold becomes fragile at 400 ℃ and higher temperatures, and producing too much CuO_x will consume Li excessively. Therefore, we set the oxidation temperature at 300 ℃.

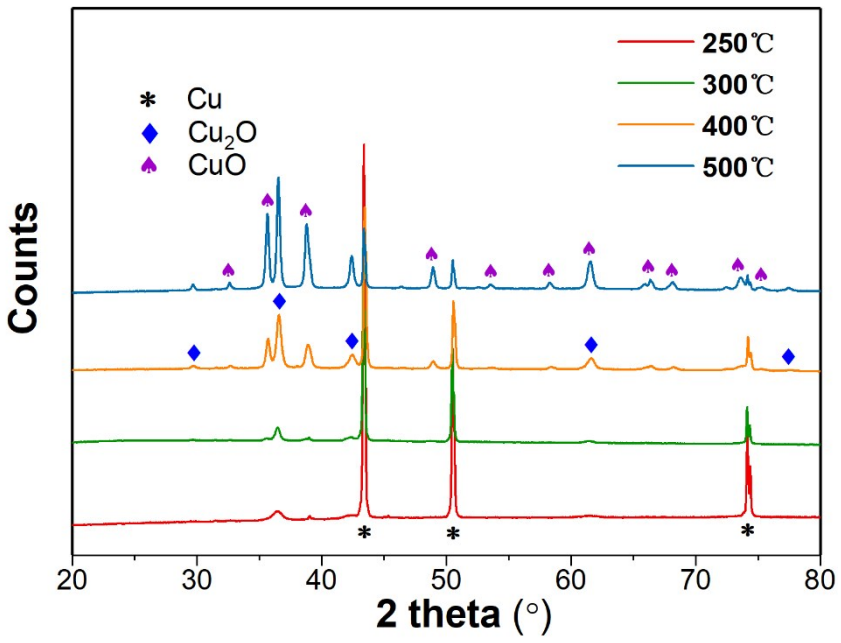

Fig. S1. The XRD patterns of the scaffold after oxidation at 250, 300, 400 and 500 ℃ for 2 h, respectively.

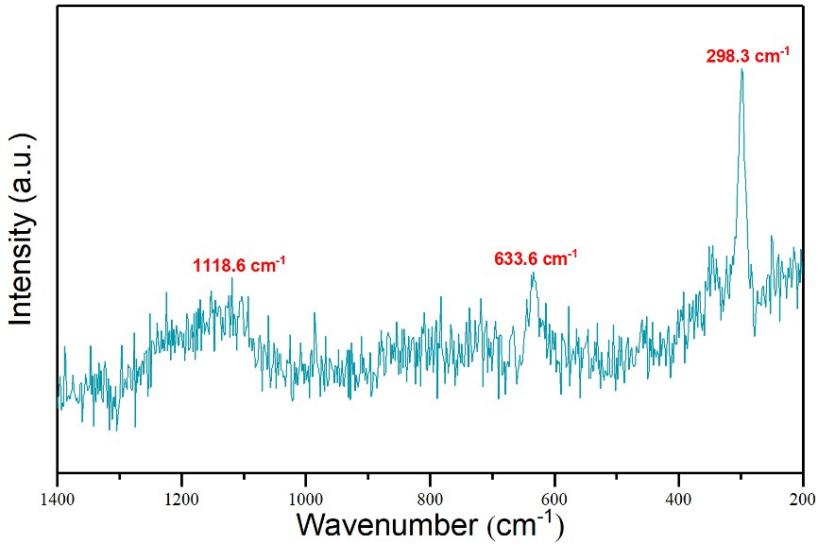

Fig. S2. The Raman spectrum of CuO_x@Cu.

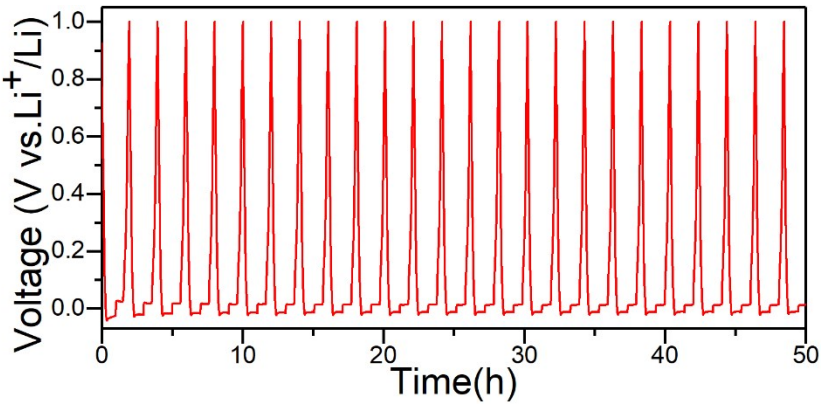

Fig. S3. The voltage-time profiles of CuO_x@Cu half cell in the 1st-25th cycles at 1 mA cm^{-2}.

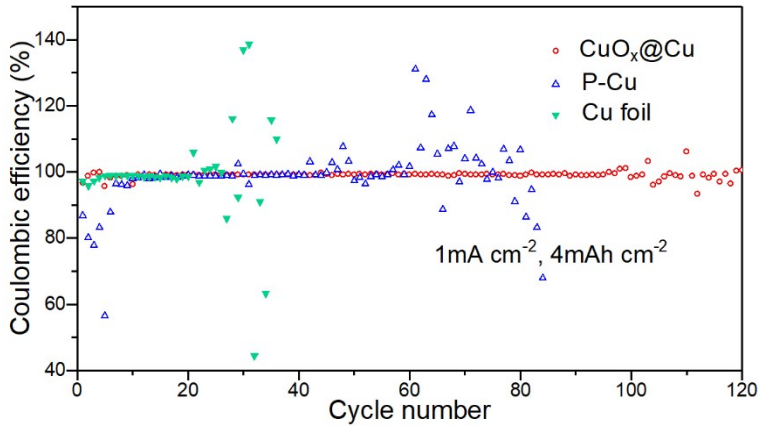

Fig. S4. The Coulombic efficiency comparison of CuO_x@Cu, P-Cu and Cu foil under the condition of 4 mAh cm^{-2} and 1 mA cm^{-2}.

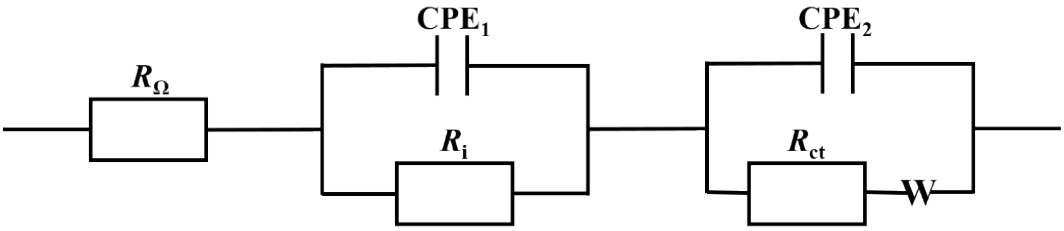

Fig. S5. The equivalent circuit diagram for **Fig. 6d** and **e**.

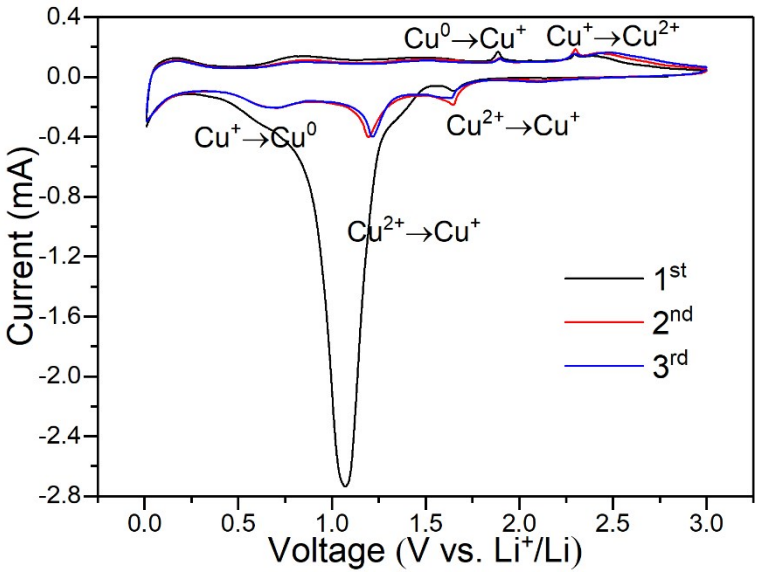

Fig. S6. The CV curves of Li//CuO_x@Cu cell between 0.01-3 V at a scan rate of 0.1 mV s^{-1}.

The details of the molten Li infusion process:

In an argon-filled glove box, a stainless steel plate was placed on the heating table, and heat up to 350 ℃ to melt Li. Then a piece of CuO_x@Cu scaffold contacted the molten Li and took in it quickly, and the molten Li could fully filled the inner space within a few seconds. Subsequently, the composite electrode cooled down and was stored in the glove box.

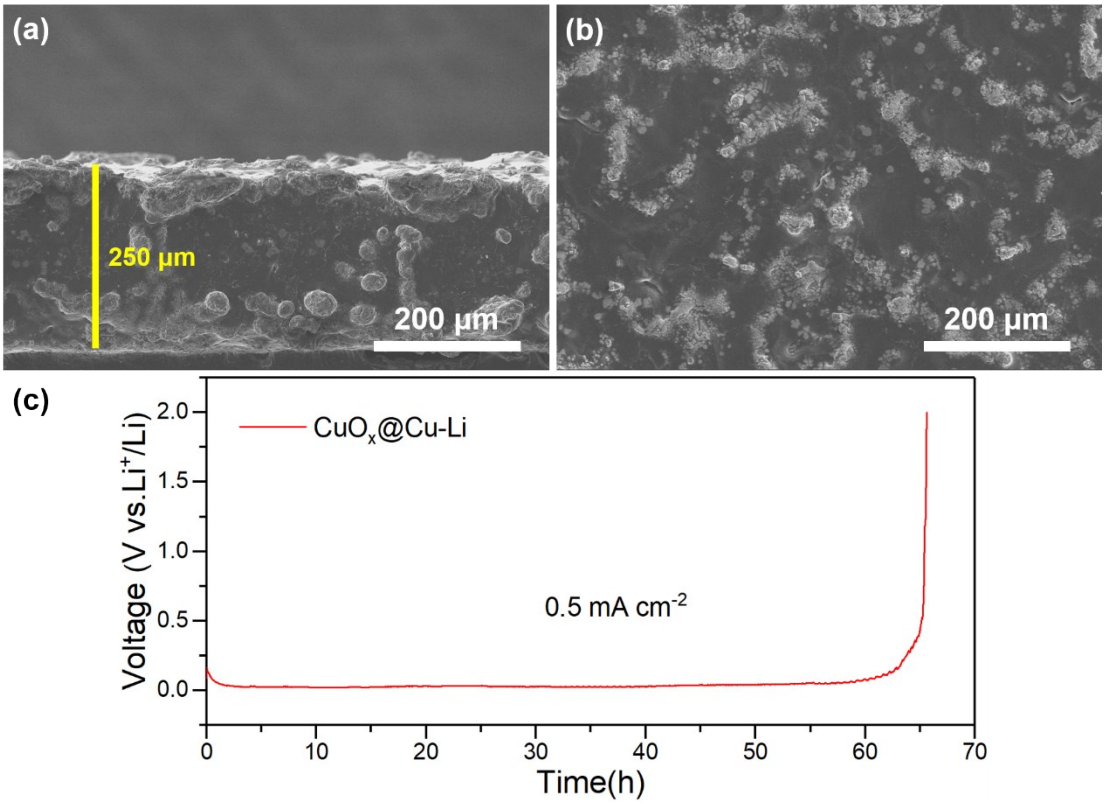

Fig. S7. (a) The cross-section image and (b) surface image of composite electrode with CuO_x@Cu and Li metal prepared by the molten Li infusion method. (c) The galvanostatic charging curve of the composite electrode at a current density of 0.5 mA cm^{-2}. The maximum capacity is calculated as 65 h × 0.5 mA cm^{-2} = 32.5 mAh cm^{-2}, and the thickness is about 250 μm, so the volumetric capacity is 32.5 ÷ 0.025 = 1300 mAh cm^{-3}.

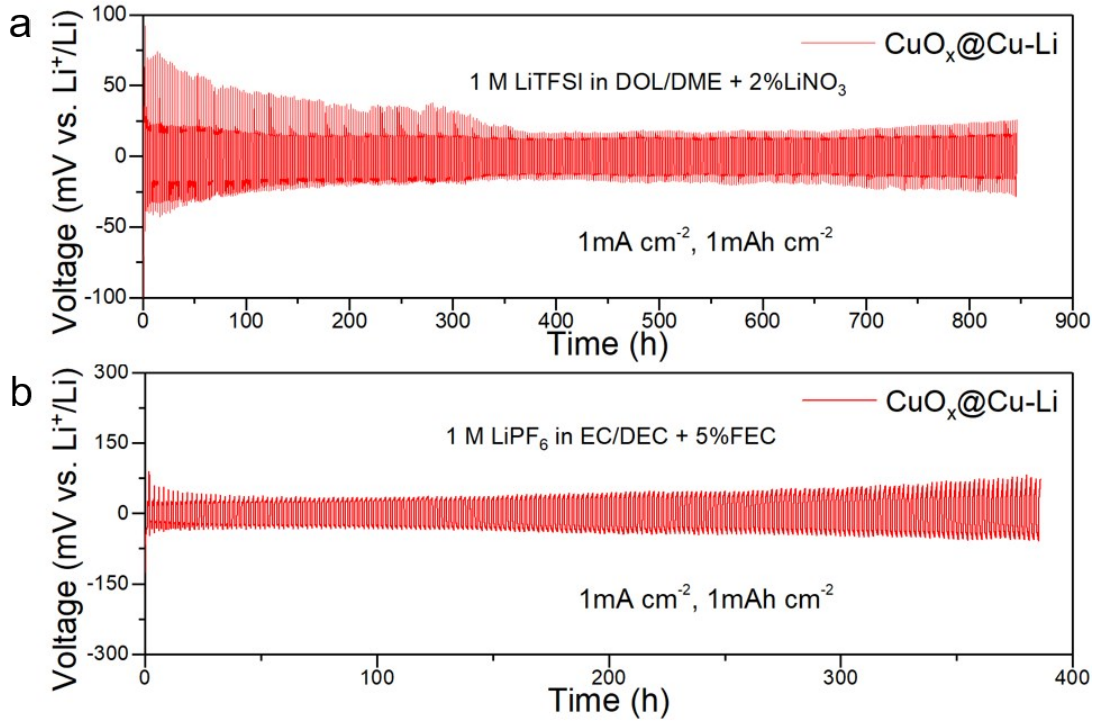

Fig. S8. The cycling performance of the CuO_x@Cu-Li (prepared by a molten Li infusion method) symmetric cell under the condition of 1 mA cm^{-2} and 1 mAh cm^{-2} in (a) the ether-based electrolyte and (b) the carbonate-based electrolyte.

Table S1. The fitted parameters for **Fig. 6d** and **e**, and the area is 0.785 cm^2.

	1st			40th		
	R_Ω (Ω cm^2)	R_i (Ω cm^2)	R_{ct} (Ω cm^2)	R_Ω (Ω cm^2)	R_i (Ω cm^2)	R_{ct} (Ω cm^2)
CuO_x@Cu	1.5	19.6	14.3	2.0	2.7	12.9
P-Cu	1.9	39.6	20.6	4.3	2.8	16.0
Cu foil	1.2	48.5	27.1	2.4	29.8	26.6

Table S2. The performance comparison of CuO_x@Cu with other reported lithiophilic scaffolds in half cells.

Materials	**Current density [mA cm^{-2}]**	**Capacity [mA h cm^{-2}]**	**Cycle number**	**Coulombic efficiency [%]**
Ni-Cu-CuO hybrid structure[2]	1	1	250	> 95
	3	1	100	> 90
Al layer coated 3D Cu[3]	0.5	2	85	~ 98.6
$Cu_{99}Zn$ alloy coated Cu[4]	0.2	0.4	400	99
	0.5	1	200	> 97
Lithiated ZnO on Cu foil[5]	1	1	200	99.2
	3	1	200	93.3
CuON nanoarray on Cu foam[6]	2	1	100	> 98
ZnO modified Ni foam[7]	1	1	300	> 98
Graphene coated Cu foam[8]	2	1	150	97.4
CuO nanosheets on Cu foil[9]	1	1	180	94

N-doped graphene-coated Ni foam[10]	1	1	200	98
This work	**1**	**1**	**>520**	**98.8**
	3	**1**	**240**	**98.4**
	5	**1**	**170**	**98.0**
	1	**4**	**120**	**99.1**

Reference

1. F. W. Young, J. V. Cathcart and A. T. Gwathmey, *Acta Metallurgica*, 1956, **4**, 145-152.
2. S. Wu, Z. Zhang, M. Lan, S. Yang, J. Cheng, J. Cai, J. Shen, Y. Zhu, K. Zhang and W. Zhang, *Adv. Mater.*, 2018, **30**.
3. H. Ye, Z. J. Zheng, H. R. Yao, S. C. Liu, T. T. Zuo, X. W. Wu, Y. X. Yin, N. W. Li, J. J. Gu, F. F. Cao and Y. G. Guo, *Angew. Chem. Int. Ed. Engl.*, 2019, **58**, 1094-1099.
4. S. Liu, X. Zhang, R. Li, L. Gao and J. Luo, *Energy Storage Mater.*, 2018, **14**, 143-148.
5. G. Wang, X. Xiong, P. Zou, X. Fu, Z. Lin, Y. Li, Y. Liu, C. Yang and M. Liu, *Chem. Eng. J.*, 2019, **378**.
6. M. Lei, Z. You, L. Ren, X. Liu and J.-G. Wang, *J. Power Sources*, 2020, **463**.
7. C. Sun, Y. Li, J. Jin, J. Yang and Z. Wen, *J. Mater. Chem. A*, 2019, **7**, 7752-7759.
8. G. Yang, J. Chen, P. Xiao, P. O. Agboola, I. Shakir and Y. Xu, *J. Mater. Chem. A*, 2018, **6**, 9899-9905.
9. C. Zhang, W. Lv, G. Zhou, Z. Huang, Y. Zhang, R. Lyu, H. Wu, Q. Yun, F. Kang and Q.-H. Yang, *Adv. Energy Mater.*, 2018, **8**.
10. R. Song, B. Wang, Y. Xie, T. Ruan, F. Wang, Y. Yuan, D. Wang and S. Dou, *J. Mater. Chem. A*, 2018, **6**, 17967-17976.